

# Planning Open and Closed-Loop Feeders with Efficiency Analysis

José L. Morillo\*, Juan F. Pérez†, Nicanor Quijano\*, and Ángela Cadena\*

\* Department of Electrical and Electronics Engineering  
Universidad de los Andes, Bogotá, Colombia

† Department of Computing  
Imperial College London, London, UK

**Abstract**—The evolution of distribution systems (DS) towards the smart-grid concept poses new challenges, triggered by the integration of distributed generation (DG) and the installation of new devices. These challenges raise the need to reconsider the traditional network operation during the planning stage, enabling the DS to be flexible to operate under different network configuration scenarios. In this paper we propose a DS planning methodology for the connection of support feeders in radial networks, explicitly considering reconfiguration options with open- and closed-loop operation. To this end, we propose an efficiency evaluation, based on Data Envelopment Analysis, to assess candidate feeders in terms of expansion costs, energy losses, and lines' chargeability, under a range of demand scenarios that include GD penetration. Additionally, we have developed a method to identify the main feeder in a radial system, obtaining a simplified version of the DS, better suited for analysis. Simulation results on a real urban DS show the effectiveness of the method to identify the best nodes in a main feeder to connect support feeders, further indicating how to divide the network into operation areas for an improved network performance.

**Index Terms**—Data envelopment analysis, Distribution system planning, Loop feeders, Efficiency evaluation.

## I. INTRODUCTION

One of the most important steps in planning the expansion and operation of distribution systems (DS) is to determine the location of fuses, reclosers, switches, and protection equipment in both the primary and lateral feeders, to achieve the required level of reliability [1]. In addition, a number of options exist to support and enhance network reliability, such as load-transfer facilities, which are used to mitigate the effects of faults in the distribution network, reconfiguring the network with open-loop and closed-loop arrangements to restore service [2]. However, under a smart-grid scheme, the DS should have the ability to continuously change the network topology, in order to maintain optimal operating conditions, including power quality, and to minimize the effects of power outages. Further, the DS design and expansion are affected by the increasing integration of distributed generation (DG), which cause congestion or power discharges in network sections, and introduce uncertainties in the power supplied by renewable sources, in addition to that of the demand behavior.

In a smart grid setting, the network is expected to be able to continuously reconfigure the feeders between open and closed-

loop arrangements. To this end, it is necessary to determine, during the planning stage, the technical feasibility of the arrangement, considering, e.g., situations of unbalanced operation, or the variations of short-circuit current and the associated modification to the protection equipment. Furthermore, it is also important to determine the operational performance of the network under multiple operating and demand scenarios, since the ability of a feeder to support the loads of other feeders during fault events depends on their utilization factors [2].

In this paper, we propose a methodology to identify the nodes in a feeder that are best suited for the connection of support feeders, considering the challenges posed by a smart-grid setting. We show how finding an optimal connection of feeders, the reliability can be considerably improved, while preserving adequate operational performance. As the DS planning problem is a nonlinear and combinatorial problem [1], we propose the use of Data Envelopment Analysis (DEA) [3] to select the best location to connect the support feeders, among a set of candidate nodes. The methodology considers open-loop operation and closed-loop arrangements, under different operating scenarios that could arise in a smart-grid scheme.

The use of DEA in the electricity industry has mostly focused on the economic efficiency evaluation of electricity distribution utilities [4], [5]. For DS planning, the use of DEA has been limited to the purely economical evaluation of expansion alternatives [6]. In this paper, we propose the use of DEA as part of a methodology to select the best location for the connection of support feeders, considering both technical and economic metrics. In particular, we evaluate alternative feeder connection in terms of reliability, expansion costs, and system operation. The proposed methodology can therefore complement existing methodologies for DS planning.

Additionally, since the evaluation of open- and closed-loop arrangements in real DSs requires the evaluation of many feasible operational scenarios, we have developed a new method to simplify the network characteristics after identifying the primary feeder, which allows us to lump together the connected loads in each lateral feeder and reflect them on the nodes in the primary feeder. This method thus simplifies the identification of candidate nodes in the primary feeder to connect support feeders. The results show how this method, together with the DEA-based evaluation, support the identification of the best nodes to connect support feeders. We have

This work has been partially supported by the ALTERNAR project, agreement 005, 07/19/13, CTel-SGR-Nariño, Colombia.

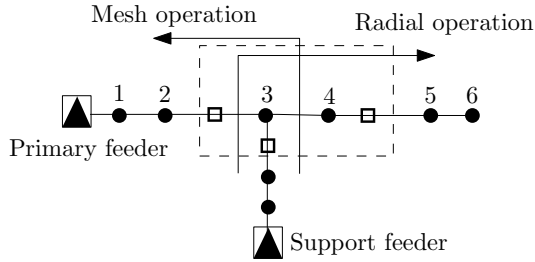


Fig. 1. Operating scenarios

found that the identified nodes can be used to split the main feeder in areas, to establish operating areas by connecting a support feeder, potentially improving service reliability and the balance power-length between areas.

## II. METHODOLOGY

Typically, open and closed-loop arrangements are designed to improve the DS reliability. In case of faults in the primary feeder, the network topology can be reconfigured by changing the state of normally open and closed switches, so that the healthy network sections can be reconnected and the faults isolated [2], [7]. As shown in Figure 1, a closed loop can be formed by connecting a support feeder in node 3 of the primary feeder, while an open loop can be formed when the switch on the branch connecting these two feeders has a normally open state. A meshed operation, where the load is served by two sources, occurs when the closed loop is established; nevertheless, a switch with normally-open state on the branch between nodes 2 and 3 implies a radial operation and a load transfer from the primary feeder to the support feeder. Many possible arrangements can be set depending on the number, state, and location of switching elements in the feeders, including cases of load transfer and load shedding.

The methodology we propose evaluates the network's ability to operate in open and closed-loop arrangements. Therefore, when the support feeder is connected to a specific node in the primary feeder, we consider a total of  $n_s$  possible scenarios, which are obtained by considering two sources of variability. First, we consider having a normally-open switch on each of the lines that compose the primary feeder, extended with the support feeder. Second, we consider a set of different demand values for the load nodes to capture demand variability and DG generation. To define the best nodes to connect the support feeder, we first identify the primary feeder and then perform a techno-economic efficiency evaluation, using DEA, as described next.

### A. Identifying the Primary Feeder

To determine the candidate nodes for the connection of, and load-transfer with, support feeders, we first need to find the DS primary feeder. The primary feeder represents the minimum set of lines where the power distributed to all loads flows. [8] introduces a matrix representation of the DS to find the primary feeder, defined as the distribution line from the substation to the farthest node to it. We extend this method to reflect the loads in each lateral feeder on the nodes in the

primary feeder. This allows us to obtain a distribution line with the length and chargeability features of the original circuit.

We make use of the mathematical formalization in [8], which represents the DS as a graph  $R = [V, E]$ , where  $V$  denotes the set of nodes, with cardinality  $n = |V|$ , including load nodes and substation nodes. The set of lines is denoted by  $E$ . A linear system  $A(R)x = b$  is defined, where  $A(R)$  is the adjacency matrix of the graph  $R$ , such that  $[A(R)]_{ij} = -1$  for  $\{(i, j) \in E\}$ ,  $[A(R)]_{ii} = 1$ , and  $[A(R)]_{ij} = 0$  otherwise.  $A \in \mathbb{R}^{n \times n}$  is an invertible matrix with linearly independent row and column vectors, since the system is assumed to be radial. On the other hand, the column vector  $b = A_2 \mathbf{1}_{n \times 1}$ , represents the lengths of each line section, where the  $(i, j)$  entry of the matrix  $A_2$  holds the length  $l_{i,j}$  of line  $(i, j) \in E$ .

Each element of the solution vector  $x_i \in x$  represents the distance from the substation to the  $i$ -th node in the DS. Therefore, the farthest node from the substation is  $i^* = \arg \max\{x(i)\}$ . Since each row of the matrix  $A(R)^{-1}$  allows us to identify the route, i.e., a set of connected nodes, from the substation to each node of the DS, the primary feeder can be represented by the vector  $v = A(R)^{-1}(i^*, \cdot)$ . Finally, we obtain the vector  $q_{PF} \in \mathbb{R}^{n \times 1}$  of equivalent loads in the primary feeder by adding the load in each lateral node to its corresponding connection node to the primary feeder. We can represent this operation by means of the Kronecker operator  $\otimes$  and the Hadamard product of matrices  $\circ$  as

$$q_{PF} = q((\mathbf{1}_{n \times 1} \otimes v) \circ A^{-1}),$$

where  $q = [q_1, q_2, \dots, q_n]^T$  is the vector of loads associated to each node of the DS.

### B. Data Envelopment Analysis (DEA)

DEA [3] is a deterministic non-parametric mathematical programming technique, which, for a set of decision-making units (DMUs), finds those that are technically efficient. This subset is called the efficient frontier. The efficiency of a DMU is measured by its ability to transform inputs into outputs [3]. In our methodology, the DMUs are the set  $F$ , with  $n_F = |F|$ , of all possible meshed networks obtained by adding a support feeder to a specific node in the primary feeder. These networks are evaluated in terms of 3 key metrics, which are obtained by considering all the  $n_s$  operating scenarios for each DMU.

For the efficiency analysis, we use the DEA CCR-I (input-oriented) model, according to which a DMU is inefficient if any of its inputs can be reduced without decreasing any output. To evaluate the potential of each DMU we consider the following three input variables: 1) capital costs,  $z_1$ ; 2) power losses,  $z_2$ ; and 3) the feeders' chargeability  $z_3$ , which combines the feeders' length and their utilization factor, and considers operational restrictions.

The measure of technical efficiency for a DMU, denoted by  $\theta$ , varies between 0 and 1, where a value of 1 indicates that no other DMU can produce the same level of output using fewer inputs. A  $DMU_0 \in F$  consumes an amount  $u_{z,0}$  of input  $z$ , and produces an amount  $y_{r,0}$  of output  $r$ . The linear-programming problem to determine the efficiency of  $DMU_0$

is [3],

$$\begin{aligned}
& \min \theta_0 = \theta \\
& \text{s.t. } \sum_{f=1}^{n_F} \lambda_f u_{z,f} \leq \theta u_{z,0} \quad z = 1, 2, \dots, Z \\
& \quad \sum_{f=1}^{n_F} \lambda_f y_{r,f} \geq y_{r,0} \quad r = 1, 2, \dots, R \\
& \quad \lambda_f \geq 0, \theta \text{ free,}
\end{aligned}$$

where  $Z$  and  $R$  are the number of inputs and outputs considered. The variable  $\lambda_f$  describes the percentage of DMU  $f$  used to construct a virtual efficient DMU to evaluate the  $DMU_0$  under analysis [3]. The variables considered for evaluation are modeled as input variables, thus we assume a dummy output of 1 for all DMUs,  $y_{1f} = 1$ .

In addition to the problem above, a second linear program is used to identify mix inefficiencies [3]. Additionally, since several DMUs can simultaneously obtain an efficiency measure of 1 in the CCR model, we use the super-efficiency model proposed in [9] to rank the efficient DMUs. To this end, the following constraint is added to the linear program above

$$\sum_{f=1, f \neq 0}^{n_F} \lambda_f = 1.$$

1) *Capital costs*: The capital costs depend on the set of line segments that make up each candidate feeder together with the main feeder. The variable  $u_1^f$  is thus given by

$$u_1^f = \sum_{(i,j) \in E} K_c l_{i,j} \frac{h(1+h)^t}{(1+h)^t - 1}, \quad \forall f = 1, 2, \dots, n_F,$$

where  $K_c$  is the annual line installation cost per unit length, assuming a single conductor type  $c$  for all lines. Here  $h$  is the discount factor and  $t$  the planning horizon in years.

2) *Power losses and Chargeability*: We define the operating scenarios, considering all the possible open and closed-loop arrangements along the main feeder. The scenarios are established by reconfiguring the network, assuming a normally-open switch on each of the lines. Next, we change the state of normally open and closed switches, to find all the possible  $n_l + 1$  scenarios for each candidate primary feeder, where  $n_l$  is the number of lines in the primary feeder. Figure 1 illustrates this step with a case where the primary feeder links two substations, as described in Section I.

In addition, we analyze different demand scenarios for each operating scenario to consider the demand variability into the analysis. Hence, we randomly generate 100 different demand values for each load node according to a uniform distribution, in an interval between the minimum and maximum peak demands expected during the planning horizon. The total number of scenarios is thus  $n_s = (n_l + 1)100$ . Further, we consider scenarios where the demand is reduced according to the percentage of DG penetration, thus considering the effects that the DG power injection could cause, such as congestion or power discharge in certain network sections. The demand at node  $i$  is thus given by

$$d_i = (d_{p_i} - d_{m_i})r + d_{m_i},$$

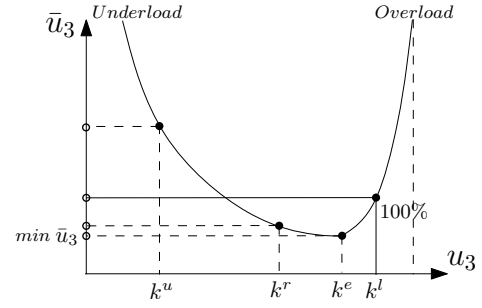


Fig. 2. Chargeability function

where  $r$  is a random number between 0 and 1, and  $d_{p_i}$  is the peak demand of load node  $i$ . The minimum demand  $d_{m_i}$  is the difference between the minimum demand without DG,  $d_{m_i}^*$ , and the available DG in node  $i$ , which is defined as a percentage  $p_i$  of the peak demand, thus  $d_{m_i} = d_{m_i}^* - p_{dg} d_{p_i}$ . Notice that  $d_{m_i}$  could be negative if the DG penetration exceeds the power requirements of the node  $i$ .

To determine the variables  $u_2$  and  $u_3$ , we perform a load flow analysis, which allows us to observe the power losses and the chargeability of the lines. As we consider a number of demand and operational scenarios for each candidate support feeder, we summarize the results of all scenarios by using the 99-th percentile of the power losses observed ( $u_2$ ), and the average chargeability ( $u_3$ ), thus

$$u_2^f = P_{99}[u_{2s}^f], \quad u_3^f = \frac{1}{n_s^f} \sum_{s=1}^{n_s^f} u_{3s}^f, \quad f = 1, \dots, n_F,$$

where  $u_{zs}^f$  is the value of the variable  $u_z$  for DMU  $f$  in scenario  $s$ .

The principle of isotonicity in DEA [3] implies that a DMU is preferred over another if it can achieve the same level of outputs than other DMUs but using fewer inputs. While this is true for variables  $u_1$  (costs) and  $u_2$  (power losses), this property does not hold for  $u_3$  (chargeability). For this variable we require an additional step, where we assume an expected chargeability level  $k^e$ , and penalize deviations away from it. The penalizing function, illustrated in Figure 2, is a convex function with minimum value when  $u_3 = k^e$ , and with a small slope between  $k^l$  and  $k^u$ , which mark values of chargeability considered acceptable. Further deviations, below  $k^l$  or above  $k^u$ , are penalized with a larger slope. The resulting value  $\bar{u}_3$  is used in DEA as it complies with the isotonicity principle.

### C. Feeder balancing

Once the support feeder has been selected based on the DEA results, we complement the methodology with the aim of ensuring reliability as measured by the energy not supplied (ENS). The ENS captures the energy not delivered to consumers as a result of system interruptions caused by failures. Since the probability of a feeder failure increases with the length of the lines, we need to a balance between length and connected load, which can be achieved by creating operation areas. In [7], the authors propose creating areas using an equivalent product  $P_L$ , which is defined, for any given area, as the product of the total power demand and the total length of

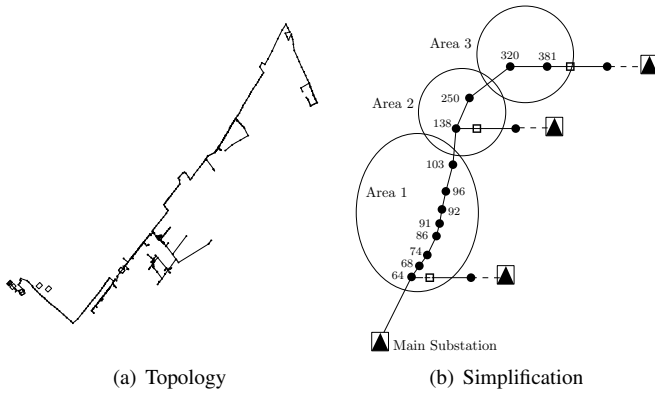


Fig. 3. Test distribution system

the lines connecting the demand nodes to the main substation. Therefore, a balance in the main feeder is achieved when high demand concentrations have a connection close to the substation, while areas with low power consumption can be far from the substation and connected through longer lines. A measure of the feeder balance,  $s_{pl}$ , is defined as the standard deviation of the product  $P_L$  across the  $n_e$  operation areas, thus

$$s_{pl}^2 = \frac{1}{n_e} \sum_{e=1}^{n_e} (P_{Le} - \bar{P}_L)^2,$$

where  $P_{Le}$  is the equivalent product for area  $e$ , and  $\bar{P}_L$  is the average value of  $P_L$  across the  $n_e$  operation areas. We thus make use of this measure to evaluate the creation of different operation areas for the support feeders selected with DEA.

### III. CASE STUDY

We apply the proposed methodology to a radial distribution system of 11.4 kV in the city of Bogotá, Colombia. The circuit has 384 nodes, with a total length of the line sections equal to 12.37 km, and a total load of 2.3 MVA. The test circuit and its simplification through the method for identifying the primary feeder are shown in Figure 3. From the results, the vector  $v$  shows that the primary feeder is made up of 237 nodes, connected by lines with a total length of 5,081 km. Further, the vector  $q_{PF}$  indicates 12 nodes that summarize well the system load. Table I displays, for each of these nodes, the aggregate load downstream of the node, for active ( $\mathbf{P}$ ) and reactive ( $\mathbf{Q}$ ) power. The column *Distance* shows the length of the connecting lines between these nodes and the substation. This simplified version of the primary feeder is the result of the first step of the methodology proposed. This can now be used to identify candidate nodes to connect support feeders in open- and closed-loop arrangements.

#### A. Efficiency evaluation

For the power flow analysis, we limit the voltage magnitude for load nodes to be between 0.95 pu and 1.05 pu, while for substations this is set at 1.00 pu. The chargeability analysis takes into account local technical standards that limit the utilization factor of the lines that make up the support feeder to be at most 85%, such that additional load can be sustained during failure events [10]. This factor is in fact  $k^e$ , the expected

TABLE I  
FEATURES OF TEST DISTRIBUTION SYSTEM

Node	P[MW]	Q[MVAR]	Distance (km)	CCR-I	SUPER-I
64	2.20	0.72	1.34	1	1.38
68	2.14	0.70	1.41	1	1.01
74	2.08	0.68	1.50	1	1.01
86	1.95	0.64	1.66	0.975	-
91	1.89	0.62	1.73	0.974	-
92	1.82	0.60	1.77	0.973	-
96	1.76	0.58	1.85	0.970	-
103	1.70	0.56	1.95	0.966	-
138	1.26	0.41	2.20	1	1.19
250	0.25	0.08	3.05	1	1.01
320	0.13	0.04	4.75	0.996	-
381	0.06	0.02	5.08	1	1.02

chargeability used to build chargeability penalizing function described in Section II-B. We also consider that the network chargeability can be above  $k^l = 100\%$  for short periods of time in contingencies. And we use the underload limit of  $k^u = 30\%$  to indicate line underuse. Finally, the demand behavior is modeled with a DG penetration rate of  $p_{dg} = 30\%$ .

As an example, we tested the connection of a feeder with the capacity to serve 100% of the demand in the test circuit. As a result, in this scenario the availability of the support feeder can avoid service interruptions caused by failures in the main substation. Table I lists the the candidate nodes for the connection of a support feeder, making up a total of 12 DMUs for efficiency analysis. We find an efficient frontier composed of 6 of these DMUs, namely, nodes 64, 68, 74, 138, 250, and 381. Notice that the the efficient DMUs are the nodes with the best technical-economic performance to connect support feeders, regarding the input variables defined. Additionally, the efficiency evaluation also provides a projection of the inefficient DMUs on the efficient frontier, indicating the level of inputs that would be necessary to make these nodes efficient.

Furthermore, 50% of the evaluated DMUs have efficiency measure of  $\theta = 1$ . Hence, we discriminate among this group with the super-efficiency model SUPER-I. The results, shown in Table I, indicate that the node 64 is the best connection alternative for support feeders, considering its operation in open- and closed-loop arrangements. However, we see from these results that another alternatives with good ranking are in the nodes 138 and 381. The topology obtained with these support feeders is shown in Figure 3(b). As the most efficient alternatives are nodes located at the beginning, end, and intermediate zones of the primary feeder, suggests the establishment of operation areas for the support feeders. To this end, we perform a feeder-balancing analysis, the third step in our methodology, to determine the best operation areas in terms of the ENS.

#### B. Feeder balancing

As mentioned before,  $P_L$  is the product between the load connected in an area and the length of the lines connecting the area to the substation. Table II shows the operation areas, the distance between the area and the substation (SE), the area load, and the resulting product  $P_L$ . The top three rows

TABLE II  
PRIMARY FEEDER AREAS AND PRODUCT  $P_L$

Area	Connection	Length(km)	P[MW]	$P_L$
64-103	SE	2.20	0.94	2.068
138-250	SE	3.05	1.13	3.446
320-381	SE	5.08	0.13	0.660
64-103	64	0.61	0.94	0.573
64-250	64	1.71	2.07	3.539
64-381	64/381	3.74	2.20	8.228
138-64	138	0.86	1.95	1.677
138-250	138	0.85	1.13	0.960
138-381	138/381	2.88	1.26	3.623
381-320	381	0.33	0.13	0.043

in Table II show the base case without support feeders, but evaluating the product  $P_L$  for three areas that can be formed with the three selected support feeders, based on their influence area, i.e., establishing the borders of each area on the nodes selected for the connection of support feeders. The balance measure  $s_{pl}$  of the base case, depicted in Table III, provides us with a benchmark to assess the impact of support feeder connection on the network balance. It is important to note that this result holds even when considering areas different from the three evaluated, because most of the load is concentrated in the middle part of the main feeder. In the bottom rows of Table II, other independent operation areas are identified together with the resulting product  $P_L$ . These areas are identified by defining the connection node as the power supply node, and the borders of each area are the nodes neighboring other supply sources, e.g., connection nodes to other support feeders, or the substation. Based on these results we can identify sets of operation areas with a smaller  $s_{pl}$ , thus more balanced and with a better ENS index.

The identified sets of operation areas are shown in Table III. The first set (64-103, 138-250, and 381-320) contains the same operation areas of the base case, but with an reduction in the imbalance measure ( $s_{pl} = 0.37$ ) of 68% compared to the base case. In this set, the connection node for the support feeder reduces the distance between the load nodes in the area and the source. We can see that the base case in fact sets an upper limit of imbalance as any scenario of open- and closed-loop arrangement can improve the balance across areas. Consequently, the ENS index in each area improves compared to the base case, thanks to the improved reliability provided by the support feeders connection. The ENS indexes are shown in Table III. A second set of areas (64-250, 138-381, and 381-138) contains larger operation areas and better balance ( $s_{pl} = 0.03$ ). However, the ENS index is higher due to the larger line length in each area.

Another consideration to take into account is that, so far, the analysis has assumed that the support feeders must have enough capacity to serve the 100% of the demand in the test circuit, but we need to consider that these support feeders may only be able to serve just a portion of that demand, since support feeders in urban areas are also expected to serve their own loads. The last column in Table III depicts the proportion of the overall covered by each area, which determines the

TABLE III  
OPERATION AREAS AND FEATURES

Area	Connection	$s_{pl}$	ENS[MWh/y]	Load(%)
Base case	SE	1.13	1.06	-
64-103	64		0.143	42.7
138-250	138	0.37	0.158	51.3
381-320	381		0.161	5.9
64-250	64		0.373	94.0
138-381	138/381	0.03	0.344	57.2

power capacity required in the support feeder. Notice that these proportions sum to more than unity because the areas overlap. Looking at the first set of operation areas, the area 138-250 concentrates half of the load. We observe that a support feeder with similar technical characteristics to the test circuit, requires a chargeability smaller than the  $k^e=85\%$  defined initially, to effectively provide power support. Similarly, the support feeders could perform their role adequately with a lower capacity, and a chargeability closer to  $k^e$ . In the second set of areas, each area covers a larger portion of the demand as it covers a wider operating range, requiring a higher power support capacity than in the first set. We therefore observe how the efficiency analysis also provides us with a guide to define the required capacity of the support feeders, which can contribute to identify better solutions.

### C. Sensitivity analysis

The chargeability function  $u_3(k^e)$ , described in Section II-B, was introduced to evaluate the circuit behavior by penalizing large deviations from an expected chargeability  $k^e$ , so that the most efficient DMUs are those closest to the function's minimum. We now perform a sensitivity analysis to see how the the efficient frontier is modified by a change in the value of  $k^e$ . To this end we use the results from the base case, modifying the input variable  $u_3$ . The resulting input variables are shown in Table IV. We observe that the input variable  $u_3$  decreases, and thus approaches the minimum of the quadratic function  $u_3(k^e)$ , as the expected chargeability  $k^e$  decreases. This result indicates that the circuit chargeability is below the expected value, and it is possible to find different alternatives for the support feeder connection by varying the  $k^e$  parameter. Figure 4 shows the change in the efficiency frontier, depicted in the space of the observed losses and chargeability. Each frontier is made up of the nodes found to be the most efficient for support feeders connection in each

TABLE IV  
INPUT VARIABLES IN DEA VARYING  $k^e$

$k^e$	60%	70%	75%	80%	85%	
<b>Node</b>	$u_2$	$u_3$	$u_3$	$u_3$	$u_3$	
64	0.16	2.30	2.92	3.24	3.68	4.21
74	0.36	2.21	2.82	3.13	3.55	4.07
108	1.31	2.00	-	-	-	-
138	2.85	1.83	2.06	2.25	2.54	2.91
250	3.59	-	2.04	2.21	2.49	2.85
320	6.25	-	2.00	2.18	-	-
381	7.09	-	2.00	2.17	2.43	2.79

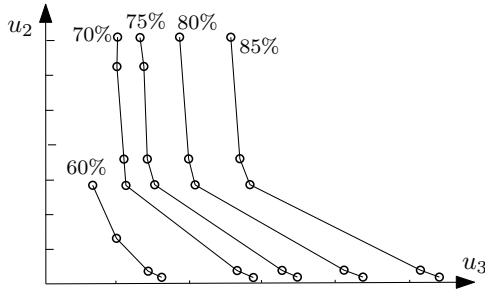


Fig. 4. DEA frontier varying the expected chargeability  $k^e$ .

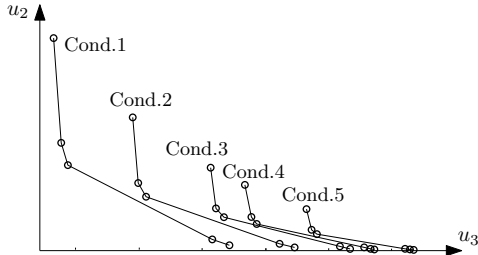


Fig. 5. DEA frontier with different conductor types.

case. The efficient frontier with  $k^e = 85\%$  is made up of five DMUs. In contrast, the frontier with  $k^e = 60\%$  conserves only three of those DMUs, as two no longer are efficient and a new one achieving efficiency only at this value of  $k^e$ . Notice how the frontiers efficiency with a smaller  $k^e$  envelop those obtained with larger values, showing how the decrease in  $k^e$  allows for configurations with less losses and chargeability deviations.

We now study the sensitivity of the efficient frontier to the conductor type selected, as this affects all the variables considered in the efficiency analysis. We evaluate five types of conductor, where type 1, used in the base case, is the cheapest and has the highest resistivity and the lowest chargeability capacity. In contrast, type 5 is the most expensive, and it has the lowest resistivity and the highest chargeability capacity. Table V shows the input variables for the 6 DMUs found efficient under all conductor types. As expected, the costs for each DMU increase with a higher conductor type, while the energy losses increase. However, it is interesting to see that the set of efficient nodes remains almost constant, with the inclusion of node 68 for conductors types 4 and 5. The change in the efficient frontier is shown in Figure 5, where we observe how the frontier associated to a smaller conductor type improves over that of a higher conductor type in the chargeability variable, but the opposite occurs with the energy losses. This is because, as mentioned above, the network operates below the expected chargeability  $k^e$ , thus showing an oversized chargeability capacity. With the different conductor types considered, new alternatives appear as options to approach the expected chargeability  $k^e$  and maintain an efficient operation.

#### IV. CONCLUSIONS

We introduced a methodology for the identification of nodes for the connection of support feeders in a DS. The

TABLE V  
INPUT VARIABLES IN DEA WITH DIFFERENT CONDUCTOR TYPES

Node	64	68	74	138	250	381	
<b>Cond.1</b>	$u_2$	0.16	-	0.36	2.85	3.59	7.09
	$u_3$	4.21	-	4.07	2.91	2.85	2.79
<b>Cond.2</b>	$u_2$	0.10	-	0.23	1.79	2.25	4.44
	$u_3$	4.72	-	4.60	3.53	3.47	3.42
<b>Cond.3</b>	$u_2$	0.06	-	0.14	1.12	1.41	2.78
	$u_3$	5.16	-	5.07	4.15	4.09	4.04
<b>Cond.4</b>	$u_2$	0.05	0.07	0.11	0.88	1.12	2.20
	$u_3$	5.35	5.32	5.27	4.42	4.37	4.32
<b>Cond.5</b>	$u_2$	0.03	0.04	0.07	0.55	0.70	1.38
	$u_3$	5.66	5.64	5.60	4.89	4.85	4.81

methodology is based on an efficiency analysis that explicitly considers operation in open- and closed-loop arrangements, thus bringing dynamic operation considerations into the DS planning stage. Additionally, we developed a method that allows us to simplify DS networks, easing the analysis of complex networks. As the result of the efficiency analysis enables the identification of operation areas, we complement the methodology with an analysis of the balance across areas and its impact on reliability. In areas where a high quality of service is expected, the open- and closed-loop arrangements increase the reliability. Nevertheless, the operation can become more complex and expensive, despite the fact that it is possible to further improve the ENS index with more sophisticated automation schemes. Finally, the results show how the technical characteristics of the DS can affect the planning decisions, and how this is captured by the efficiency analysis.

#### REFERENCES

- [1] H. Lee Willis, *Power Distribution Planning Reference Book 2nd Edition*. CRC Press, March 2004.
- [2] T.-H. Chen, W.-T. Huang, J.-C. Gu, G.-C. Pu, Y.-F. Hsu, and T.-Y. Guo, "Feasibility study of upgrading primary feeders from radial and open-loop to normally closed-loop arrangement," *IEEE Transactions on Power Systems*, vol. 19, no. 3, pp. 1308–1316, Aug 2004.
- [3] W. Cooper, L. Seiford, and K. Tone, *Data Envelopment Analysis: A Comprehensive Text with Models, Applications, References and DEA-Solver Software*. Springer, 2007.
- [4] D. Giannakis, T. Jamasb, and M. Pollitt, "Benchmarking and incentive regulation of quality of service: an application to the UK electricity distribution utilities," Faculty of Economics, University of Cambridge, Cambridge Working Papers in Economics 0408, Jan. 2004.
- [5] R. Sanhueza, H. Rudnick, and H. Lagunas, "DEA efficiency for the determination of the electric power distribution added value," *IEEE Transactions on Power Systems*, vol. 19, no. 2, pp. 919–925, May 2004.
- [6] D.-C. Wang, L. Ochoa, and G. Harrison, "Modified GA and data envelopment analysis for multistage distribution network expansion planning under uncertainty," *IEEE Transactions on Power Systems*, vol. 26, no. 2, pp. 897–904, May 2011.
- [7] M.-C. Alvarez-Herault, D. Picault, R. Caire, B. Raison, N. HadjSaid, and W. Bienia, "A novel hybrid network architecture to increase DG insertion in electrical distribution systems," *IEEE Transactions on Power Systems*, vol. 26, no. 2, pp. 905–914, May 2011.
- [8] D. M. B. S. De Souza, A. F. De Assis, I. da Silva, and W. Usida, "Efficient fuzzy approach for allocating fault indicators in power distribution lines," in *2008 IEEE/PES Transmission and Distribution Conference and Exposition: Latin America*, Aug 2008.
- [9] P. Andersen and N. C. Petersen, "A procedure for ranking efficient units in data envelopment analysis," *Manage. Sci.*, vol. 39, no. 10, pp. 1261–1264, Oct. 1993.
- [10] *Crterios de Planificaci3n de la Red El3ctrica de Media Tensi3n*. Endesa-Colombia, 2011.